Comprehensive and Accurate Control of Thermosensitivity of Poly(2-alkyl-2-oxazoline)s via Well-Defined Gradient or Random Copolymerization

Joon-Sik Park[†] and Kazunori Kataoka*[,†,‡,§]

Department of Materials Engineering, Graduate School of Engineering, The University of Tokyo, 7-3-1 Hongo, Bunkyo-ku, Tokyo 113-8656, Japan, Center for Disease Biology and Integrative Medicine, Graduate School of Medicine, The University of Tokyo, Tokyo 113-0033, Japan, and Center for NanoBio Integration, The University of Tokyo, 7-3-1 Hongo, Bunkyo-ku, Tokyo 113-8656, Japan

Received January 16, 2007; Revised Manuscript Received March 10, 2007

ABSTRACT: The lower critical solution temperature (LCST) of the poly(2-alkyl-2-oxazoline)s (POx) was precisely tuned over a broad range of temperatures via the well-defined gradient or random copolymerization between 2-*n*-propyl-2-oxazoline (*n*PrOx) and either 2-isopropyl-2-oxazoline (*i*PrOx) or 2-ethyl-2-oxazoline (EtOx). All the copolymerizations were cationically initiated by methyl *p*-tosylate at the optimum condition (42 °C in acetonitrile) for the living polymerization, resulting in an extremely narrow molecular weight distribution ($M_w/M_n \leq 1.05$). It was determined from the composition analysis by ^{1}H NMR and MALDI−TOF mass spectrometry that the respective monomer reactivity ratios were found to be 3.15 and 0.57 for *n*PrOx and *i*PrOx, respectively, sufficiently different to form the gradient copolymers P(*n*PrOx-*grad*-*i*PrOx), and 1.28 and 1.04 for *n*PrOx and EtOx, respectively, indicating the favorable formation of the random copolymers P(*n*PrOx-*ran*-EtOx). Both gradient and random copolymers followed a simple and practical rule during their LCST modulation, depending on the compositional variation between the hydrophilic/hydrophobic 2-alkyl-2-oxazoline monomers centering on the *i*PrOx. In particular, it was found that poly(2-*n*-propyl-2-oxazoline) (P*n*PrOx) independently exhibited a sharp LCST behavior near room temperature, even comparable to that of poly(2-isopropyl-2-oxazoline) (P*i*PrOx). Furthermore, the P(*n*PrOx-*ran*-EtOx) copolymers were not only synthesized much faster than the gradient copolymers with the *i*PrOx component but also showed a clear phase transition behavior over the wide temperature range from 23.8 to 75.1 °C, offering the most ideal choice, viz., a simple random distribution of the two monomers for tuning the LCST.

Introduction

A great deal of attention has focused on the so-called "smart" polymeric materials showing a discrete change in their propensity that respond to external physical and chemical stimuli, including light, temperature, pH, and magnetic and electric fields. In particular, temperature-responsive polymers are considered useful for various practical applications, such as supports for catalysts,[1] sensors,[2] separation systems,[3] enzymatic bioconjugates,[4] and drug carriers.[5] Drastic changes in the solubility, turbidity, and other physicochemical properties of thermosensitive polymers can be simply induced by adding or removing heat energy, and such feasibility is especially important when designing "smart" polymeric materials that respond to the external stimuli. At this time, careful engineering of the polymer structure should be inevitable in order to realize the precise modulation of the responding temperature as well as the transition sharpness.

In this regard, we have recently established the controlled synthetic route of novel end-functionalized thermosensitive poly(2-isopropyl-2-oxazoline) (P*i*PrOx) telechelics at the optimum condition (42 °C in acetonitrile).[6] The notable LCST-type transition behaviors of P*i*PrOx, characterized by a fast responsivity comparable to the conventional poly(*N*-isopropylacrylamide) (PNiPAAm),[7] could be achieved by the precise control of the well-defined polymeric structures with appreciably narrow molecular weight distributions (MWD) through the living polymerization mechanism. For the development of a thermosensitive drug carrier, P*i*PrOx-based polyion complex (PIC) micelles were also prepared via the complexation of a pair of oppositely charged block ionomers.[8] The PIC micelles exhibited a sharp and constant LCST of 32 °C regardless of the total concentration, demonstrating that the precise control of the polymer structure, such as the molecular weight, MWD, and end group was closely related to the characteristic phase transition behavior of the hierarchal self-assembly like polymeric micelles. Furthermore, the LCST of P*i*PrOx was able to be finely tuned by incorporating the specific composition of the hydrophilic 2-ethyl-2-oxazoline monomer units within the main chains, mainly considering the biorelated application with a LCST near the physiological conditions.[9] In that system, the oxazoline monomers of 2-isopropyl-2-oxazoline and 2-ethyl-2-oxazoline had sufficiently different reactivity ratios of 1.78 and 0.79, respectively, thus offering a useful route to engineer thermosensitive gradient copolymers with an extremely narrow MWD ($M_w/M_n \leq 1.02$).

For now, it is well-known that the length of the alkyl substituents of the poly(2-alkyl-2-oxazoline)s (POx) determines to a large extent their relative hydrophilicity, and only a few 2-alkyl-2-oxazolines (Ox), such as the 2-methyl-, 2-ethyl-, and 2-isopropyl-2-oxazolines, lead to the good solubility of their respective polymers in water at room temperature.[10] Curiously, in the case of the poly(2-ethyl-2-oxazoline) (PEtOx) high polymers with molecular weights above ∼20 000, their LCST

* Corresponding author. Telephone: +81-3-5841-7138. Fax: +81-3-5841-7139. E-mail: kataoka@bmw.t.u-tokyo.ac.jp.
† Department of Materials Engineering, Graduate School of Engineering, The University of Tokyo.
‡ Center for Disease Biology and Integrative Medicine, Graduate School of Medicine, The University of Tokyo.
§ Center for NanoBio Integration, The University of Tokyo.

10.1021/ma0701181 CCC: $37.00
Published on Web 04/20/2007

Scheme 1. Synthetic Schemes for the Gradient Copolymerization of *n*PrOx and *i*PrOx and the Random Copolymerization of *n*PrOx and EtOx

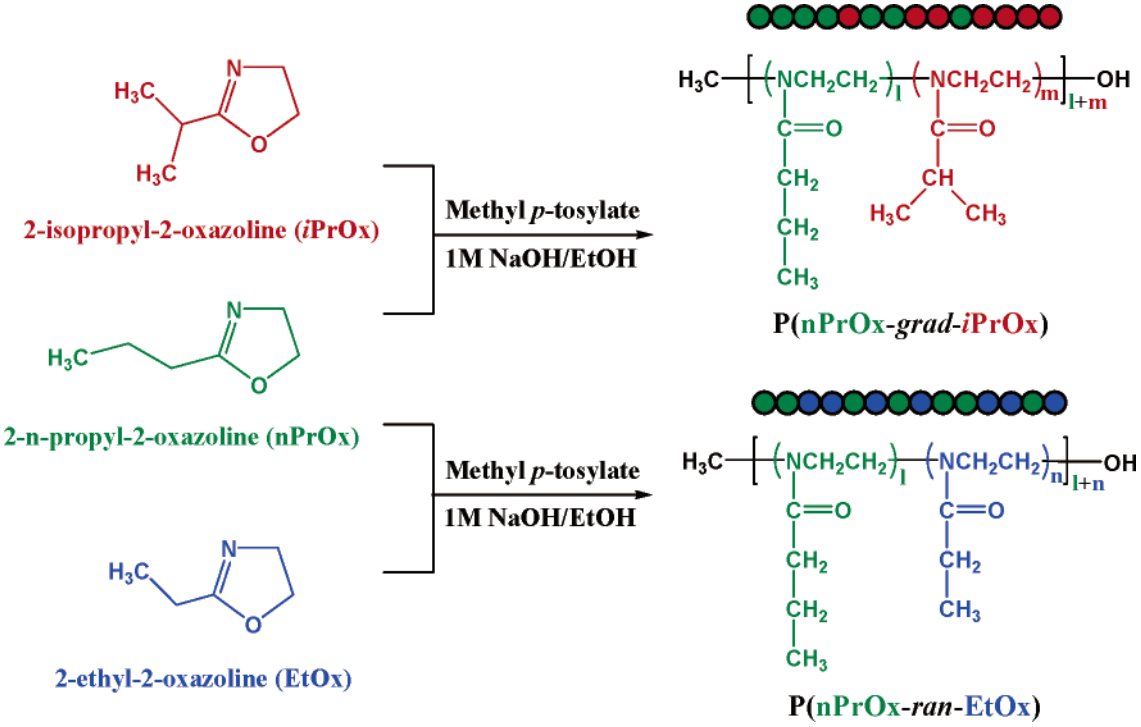

values were observed around 62−65 °C depending on molecular weight and concentration, much higher than that of P*i*PrOx.[11] In this respect, we also focused on the poly(2-*n*-propyl-2-oxazoline) (P*n*PrOx) which has one more hydrophobic methylene group in the side 2-position compared to PEtOx as well as becomes a chemical isomer of P*i*PrOx. Although there is an example investigating the property of the P*n*PrOx-based lipogel (organogel) swollen in organic solvents,[12] the solution properties of the P*n*PrOx oligomers have not yet been studied, especially in terms of their temperature-induced phase transition behavior in water. Moreover, little attention has been paid to the LCST control of POx copolymers except for our recent gradient system, though there are various hydrophobic and hydrophilic Ox monomers such as *n*PrOx, *i*PrOx, and EtOx. Thus, it was highly motivating that a variety of combinations between two Ox monomers with different or similar reactivity ratios could selectively produce the thermosensitive gradient or random POx copolymers according to particular applications.

In this study, we have accomplished the accurate control of the LCST in the POx system over a wide range of temperature by obtaining the well-defined gradient or random copolymers via the selective combination between *n*PrOx and either *i*PrOx or EtOx (Scheme 1). Of special interest is the P*n*PrOx homopolymer independently exhibiting a sharp LCST-type phase transition behavior around 23.8 °C, even comparable to that of P*i*PrOx. To the best of the author's knowledge, this is the first example proving that P*n*PrOx was also soluble in an aqueous solution as well as having a clear thermosensitivity near room temperature. Furthermore, the copolymers composed of *n*PrOx and EtOx resulted in a fully random composition, and also showed a rapid and modulated response to the temperature change from 23.8 to 75.1 °C, considered the most ideal system for tuning the LCST.

Experimental Section

Materials. 2-Isopropyl-2-oxazoline (*i*PrOx) was synthesized from isobutyric acid (Wako Pure Chemical Industries, Ltd., Osaka, Japan) and 2-aminoethanol (Wako Pure Chemical Industries) as previously described.[6] Methyl *p*-tosylate (MeOTs) (Tokyo Kasei Kogyo Co., Ltd., Tokyo, Japan) was distilled from calcium hydride under reduced pressure. 2-Ethyl-2-oxazoline (EtOx) (Aldrich Chemical Co., Ltd., Milwaukee, WI), 2-*n*-propyl-2-oxazoline (*n*PrOx) (Aldrich Chemical Co., Ltd.), and acetonitrile (Wako Pure Chemical Industries) were distilled from calcium hydride following conventional procedures.[13] All other chemicals were used without further purification.

Techniques. The ^{1}H NMR spectra were recorded using a JEOL EX 300 spectrometer at 300 MHz. The chemical shifts were reported in parts per million (ppm) downfield from tetramethylsilane. The molecular weights and molecular weight distributions were determined using a GPC (TOSOH HLC-8220) system equipped with two TSK gel columns (G4000H$_{HR}$ & G3000H$_{HR}$ and SuperAW4000 & SuperAW3000) and an internal refractive index (RI) detector. The columns were eluted with DMF containing lithium bromide (10 mM) and triethylamine (30 mM) at the flow rate of 0.8 mL/min and were maintained at a temperature of 40 °C. The molecular weights (MW) were calibrated using poly(2-isopropyl-2-oxazoline) (P*i*PrOx) standards of which the absolute molecular weights were determined by MALDI−TOF mass spectrometry (Me−P*i*PrOx−OH; MW$_{TOF-MS}$ = 5400, 8700, 11500, 17000). The mass measurements were performed using a MALDI−TOF mass spectrometer (Bruker REFLEX III) operating at an acceleration voltage of 23 kV in the reflection mode. The UV−vis spectra were obtained using a V-550 UV/vis JASCO spectrophotometer.

Synthesis of Homopolymers. The synthetic results of poly(2-isopropyl-2-oxazoline) (P*i*PrOx) and poly(2-ethyl-2-oxazoline) (PEtOx) homopolymers having hydroxyl groups at the ω-terminal ends were taken from our recent account unless otherwise stated.[9]

Poly(2-*n*-propyl-2-oxazoline) (P*n*PrOx) Having a Hydroxyl Group at the ω-Terminal End. 2-*n*-Propyl-2-oxazoline (*n*PrOx) (5.0 g, 44.2 mmol) was added via syringe to a solution of methyl *p*-tosylate (MeOTs) (0.093 g, 0.50 mmol) in acetonitrile (15 mL). The polymerization mixture was stirred at 42 °C for 162.3 h under an argon atmosphere. The mixture was then cooled to room temperature, then treated with methanolic NaOH (1 M) to introduce a hydroxyl group at one of the chain ends (Me−P*n*PrOx−OH).

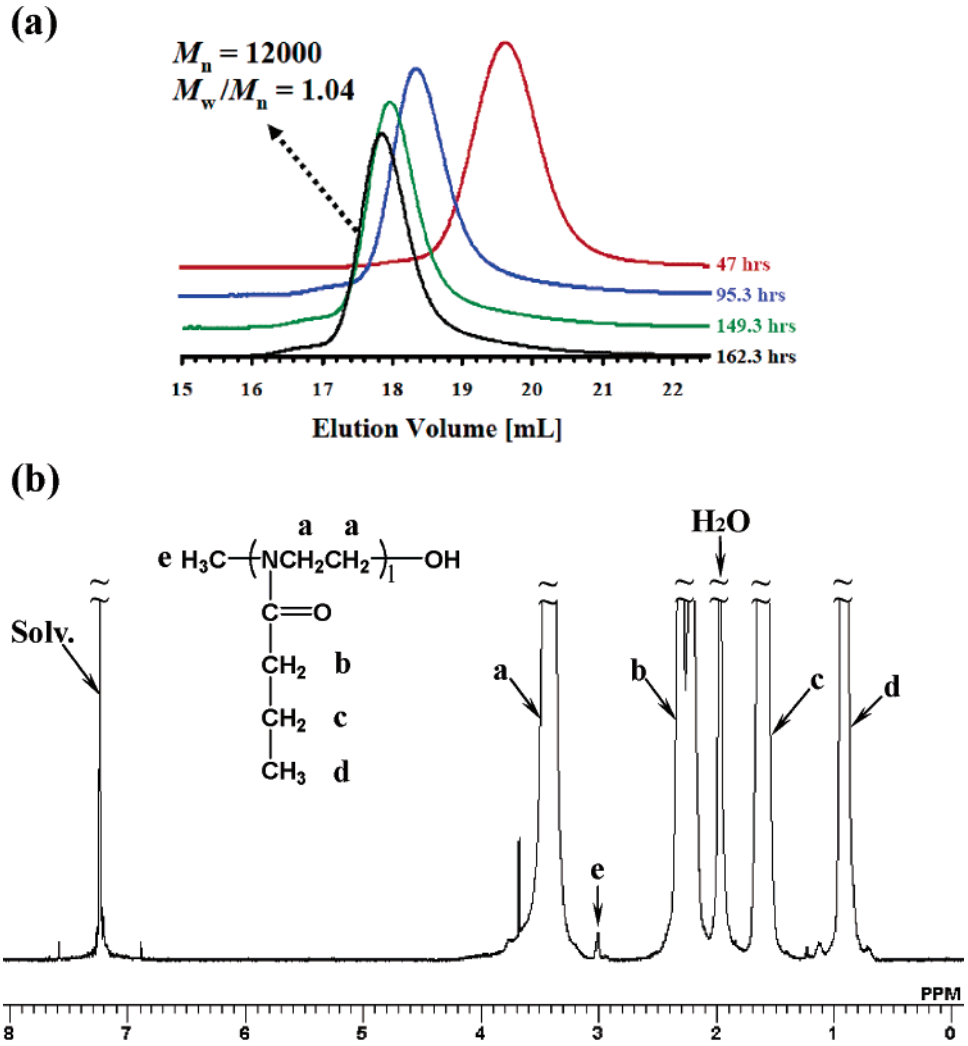

Figure 1. (a) GPC traces of ω-hydroxyl terminated P*n*PrOx homopolymers (Me−P*n*PrOx−OH) with different molecular weights (column, G4000H_{HR} and G3000H_{HR}; P*i*PrOx standard; eluent, DMF (containing 10 mM LiCl and 30 mM TEA); temperature, 40 °C; RI detection) and (b) ^{1}H NMR spectrum of Me−P*n*PrOx−OH in $CDCl_3$ at 25 °C.

Table 1. Gradient Copolymerization Results between *n*PrOx and *i*PrOx at Different Feed Compositions[a] and Their T_{cp} Values

feed ratio (*n*PrOx:*i*PrOx)	yield (%)	M_n (M_w/M_n) MALDI−TOF MS[b]	M_n (M_w/M_n) GPC[c]	*l*:*m*[d]	T_{cp}[e] (°C)
100:0	94	10800 (1.04)	12000 (1.04)	100:0	23.8
75:25	80	11100 (1.01)	13300 (1.03)	80:20	26.3
50:50	88	11400 (1.01)	12300 (1.02)	54:46	30.1
25:75	84	10100 (1.01)	12300 (1.02)	33:67	33.8
0:100	90	10200 (1.01)	9700 (1.02)	0:100	38.7

[a] Reaction conditions: ([*n*PrOx] + [*i*PrOx])/$[MeOTs]_{init.}$ = 88.4, $[MeOTs]_{init.}/[CH_3CN]_{solv.}$ = 0.031 mol/L, 42 °C, terminated with methanolic NaOH (1 M) for hydroxyl ω-end group. [b] Bruker REFLEX III, operating at an acceleration voltage of 23 kV in the reflection mode. [c] DMF (10 mM LiCl and 30 mM TEA), 40 °C, RI detection. [d] Determined by ^{1}H NMR spectroscopy for the final (co)polymer products (monomer composition: *l* = [*n*PrOx], *m* = [*i*PrOx]). [e] Measured by UV−vis spectroscopy (*c* = 1.0 wt %).

Table 2. Random Copolymerization Results between *n*PrOx and EtOx at Different Feed Compositions[a] and Their T_{cp} Values

feed ratio (*n*PrOx:EtOx)	yield (%)	M_n (M_w/M_n) MALDI−TOF MS[b]	M_n (M_w/M_n) GPC[c]	*l*:*n*[d]	T_{cp}[e] (°C)
100:0	94	10800 (1.04)	12000 (1.04)	100:0	23.8
75:25	95	11000 (1.01)	12900 (1.02)	74:26	36.3
50:50	90	10000 (1.01)	12400 (1.02)	53:47	41.8
25:75	88	14000 (1.01)	14000 (1.05)	32:68	50.6
5:95	91	10100 (1.01)	10200 (1.04)	9:91	75.1
0:100	95	8300 (1.01)	8000 (1.02)	0:100	

[a] Reaction conditions: ([*n*PrOx] + [EtOx])/$[MeOTs]_{init.}$ = 88.4, $[MeOTs]_{init.}/[CH_3CN]_{solv.}$ = 0.031 mol/L, 42 °C, terminated with methanolic NaOH (1 M) for hydroxyl ω-end group. [b] Bruker REFLEX III, operating at an acceleration voltage of 23 kV in the reflection mode. [c] DMF (10 mM LiCl and 30 mM TEA), 40 °C, RI detection. [d] Determined by ^{1}H NMR spectroscopy for the final (co)polymer products (monomer composition: *l* = [*n*PrOx], *n* = [EtOx]). [e] Measured by UV−vis spectroscopy (*c* = 1.0 wt %).

The solution of Me−P*n*PrOx−OH was purified via dialysis for 2 days against distilled water and then recovered by lyophilization. Several samples were collected during the course of the polymerization and subjected to the same treatment. The conversion yield and structure of the polymers were analyzed by GPC and ^{1}H NMR spectroscopy (total yields: 4.7 g, 94%).

Synthesis of Gradient Copolymers (P*n*PrOx$_{25\%}$*i*PrOx$_{75\%}$, P*n*PrOx$_{50\%}$*i*PrOx$_{50\%}$, P*n*PrOx$_{75\%}$*i*PrOx$_{25\%}$) Having a Hydroxyl Group at the ω-Terminal End. The respective mixtures of 2-*n*-propyl-2-oxazoline (*n*PrOx$_{25\%}$ = 0.625 g, 5.53 mmol; *n*PrOx$_{50\%}$ = 1.25 g, 11.1 mmol; *n*PrOx$_{75\%}$ = 1.88 g, 16.6 mmol) and 2-isopropyl-2-oxazoline (*i*PrOx$_{75\%}$ = 1.88 g, 16.6 mmol; *i*PrOx$_{50\%}$ = 1.25 g, 11.1 mmol; *i*PrOx$_{25\%}$ = 0.625 g, 5.53 mmol) were added to a solution of MeOTs (0.0465 g, 0.250 mmol) in acetonitrile (8 mL). The polymerization mixture was stirred at 42 °C for 378 h (P*n*PrOx$_{25\%}$*i*PrOx$_{75\%}$), 308.5 h (P*n*PrOx$_{50\%}$*i*PrOx$_{50\%}$), and 206.8 h (P*n*PrOx$_{75\%}$*i*PrOx$_{25\%}$) under an argon atmosphere, respectively. The

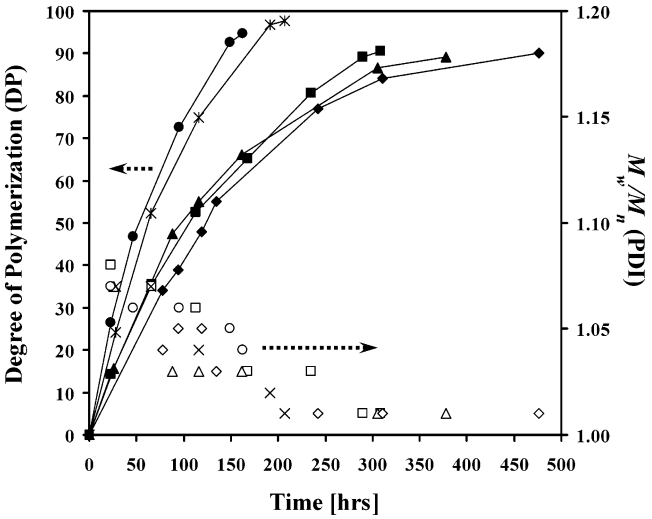

Figure 2. Degree of polymerization (DP) (left ordinate, symbols with dashed lines) and polydispersity index (PDI) (right ordinate), obtained from MALDI−TOF mass spectrometry, vs reaction time for two homopolymers (P*n*PrO*x* (●, ○), P*i*PrOx (◆, ◇)) and three gradient copolymers (P*n*PrO$x_{25\%}$*i*PrO$x_{75\%}$ (▲, △), P*n*PrO$x_{50\%}$*i*PrO$x_{50\%}$ (■, □), and P*n*PrO$x_{75\%}$*i*PrO$x_{25\%}$ (∗, ×)).

reaction mixtures were cooled to room temperature, and then treated with methanolic NaOH (1 M) to introduce a hydroxyl group at one of the chain ends. The copolymer solutions were purified via dialysis for 2 days against distilled water and then recovered by lyophilization. Several samples of the respective copolymers were collected during the course of the copolymerization. They were subjected to the same treatment as described above, and analyzed by GPC, MALDI−TOF mass, and ^{1}H NMR spectrometers in order to determine the conversion yield and composition of the copolymers (total yields: 2.1 g, 84% (P*n*PrO$x_{25\%}$*i*PrO$x_{75\%}$); 2.2 g, 88% (P*n*PrO$x_{50\%}$*i*PrO$x_{50\%}$); 2.0 g, 80% (P*n*PrO$x_{75\%}$*i*PrO$x_{25\%}$)).

Synthesis of Random Copolymers (P*n*PrO$x_{5\%}$EtO$x_{95\%}$, P*n*PrO$x_{25\%}$EtO$x_{75\%}$, P*n*PrO$x_{50\%}$EtO$x_{50\%}$, P*n*PrO$x_{75\%}$EtO$x_{25\%}$) Having a Hydroxyl Group at the ω-Terminal End. The respective mixtures of 2-*n*-propyl-2-oxazoline (*n*PrO$x_{5\%}$ = 0.126 g, 1.11 mmol; *n*PrO$x_{25\%}$ = 0.626 g, 5.53 mmol; *n*PrO$x_{50\%}$ = 1.250 g, 11.1 mmol; *n*PrO$x_{75\%}$ = 1.873 g, 16.6 mmol) and 2-ethyl-2-oxazoline (EtO$x_{95\%}$ = 2.081 g, 21.0 mmol; EtO$x_{75\%}$ = 1.642 g, 16.6 mmol; EtO$x_{50\%}$ = 1.095 g, 11.1 mmol; EtO$x_{25\%}$ = 0.548 g, 5.53 mmol) were added to a solution of MeOTs (0.0465 g, 0.250 mmol) in acetonitrile (8 mL). The polymerization mixture was stirred at 42 °C for 264.5 h (P*n*PrO$x_{5\%}$EtO$x_{95\%}$), 200 h (P*n*PrO$x_{25\%}$EtO$x_{75\%}$), 235.5 h (P*n*PrO$x_{50\%}$EtO$x_{50\%}$), and 200 h (P*n*PrO$x_{75\%}$EtO$x_{25\%}$) under an argon atmosphere, respectively. The reaction mixtures were cooled to room temperature, and then treated with methanolic NaOH (1 M) to introduce a hydroxyl group at one of the chain ends. The copolymer solutions were purified via dialysis for 2 days against distilled water and then recovered by lyophilization. Several samples of the respective copolymers were collected during the course of the copolymerization. They were subjected to the same treatment as described above, and analyzed using MALDI−TOF mass and ^{1}H NMR spectrometers in order to determine the conversion yield and composition of the copolymers (total yields: 2.0 g, 91% (P*n*PrO$x_{5\%}$EtO$x_{95\%}$); 2.0 g, 88% (P*n*PrO$x_{25\%}$EtO$x_{75\%}$); 2.1 g, 90% (P*n*PrO$x_{50\%}$EtO$x_{50\%}$); 2.3 g, 95% (P*n*PrO$x_{75\%}$EtO$x_{25\%}$)).

MALDI−TOF Mass Spectrometry. An external calibration was performed using poly(2-isopropyl-2-oxazoline) standards (Me−P*i*PrOx−OH; MW = 5400, 8700, 11500, 17000). Ions were generated by laser desorption at 337 nm (N_2 laser, 3 ns pulse width, 10^6−10^7 W/cm^2). For each spectrum, approximately 400 transients were accumulated and all spectra were recorded in the reflection mode. The data evaluation was performed with the Bruker XMASS program using the reflection spectra only in order to achieve a better signal-to-noise ratio. α-Cyano-4-hydroxycinnamic acid (CCA) (Fluka) was selected as a suitable matrix. A trifluoroacetic acid/acetonitrile (0.1% TFA:CH_3CN = 2:1) solution of CCA (10 mg/mL) was mixed with a solution of the polymer in acetonitrile (1 mg/mL) at an equimolar ratio. The resulting mixture was shaken for a few seconds. An aliquot of the mixture (1 μL) was placed on the target plate and inserted into the ion source chamber after being slowly dried. The polymer concentration of the polymer/matrix mixture solution could be diluted for the optimum ionization with an acetone solution of CCA (10 mg/mL).

Turbidity Measurements. Cloud points were determined by spectrophotometric detection of the changes in transmittance (λ = 500 nm) of the aqueous polymer solutions (1.0 wt %) heated at a constant rate (0.5 °C/min). The samples were placed in a temperature-controlled circulating water bath. The cloud point values of the polymer solutions were determined as the temperature corresponding to a 10% decrease in the optical transmittance.

Results and Discussion

Synthesis of Poly(2-*n*-propyl-2-oxazoline) (P*n*PrOx). Prior to the synthesis of a series of gradient and random copolymers, the kinetic behavior of the P*n*PrOx homopolymer was compared with those of P*i*PrOx and PEtOx under identical reaction conditions. To avoid the spontaneously occurring side reactions, such as chain transfer and coupling,[14] all the polymerizations of the respective Ox monomers (*n*PrOx, *i*PrOx, and EtOx) were conducted under mild temperature conditions (42 °C in acetonitrile).

The cationic ring-opening polymerization of *n*PrOx, initiated with MeOTs in acetonitrile, was done to obtain the poly(2-*n*-propyl-2-oxazoline) carrying a hydroxyl group at the ω-end (Me−P*n*PrOx−OH) under a mild temperature condition (42 °C). After the polymerization was left to proceed for ca. 162.3 h, it was ascertained from the GPC diagrams (Figure 1a) that the time-dependent change in the number-average molecular weight (M_n) and the molecular weight distribution were almost consistent with the living polymerization process; for the final product, the polydispersity index was low (PDI $_{GPC}$ = 1.04, PDI_{TOF-MS} = 1.04) and the experimental M_n value ($M_{n,GPC}$ = 12 000, $M_{n,TOF-MS}$ = 10 800) was close to the value predicted from the initial monomer/initiator ratio [$M_{n,calcd}$ = 10 000] (Tables 1 and 2). The ^{1}H NMR spectrum of Me−P*n*PrOx−OH in $CDCl_3$ (Figure 1b) presented a broad singlet at δ 3.39 ppm attributed to the resonance of the methylene protons on the polymer backbone, a broad singlet at δ 0.90 ppm ascribed to the resonance of the methyl protons of the *n*-propyl group on the polymer side chain, and a singlet at δ 3.01 ppm due to the resonance of the α-terminal methyl protons. However, in the case of the P*n*PrOx polymerization, the side reactions, such as chain transfer and coupling, were slightly more pronounced than the other POx systems, such as P*i*PrOx and PEtOx, as seen from the GPC charts with a lower molecular weight tailing and a higher molecular weight shoulder. It was likely that the pK_a values of the methine (CH) at the 2-isopropyl group of *i*PrOx and the methylene (CH_2) at the 2-*n*-propyl group of *n*PrOx and the 2-ethyl group of EtOx in proximity to the cationic oxazolinum ring were related to the difficulty level of proton abstraction by the *p*-tosylate anion. This assumption could be supported by applying Hammett's substituent constant (σ) values taken from a conventional reference.[15] It was thus calculated to be $\sigma_{i\mathrm{Pr}}$ = −0.340 for CH at the 2-isopropyl group with two CH_3, $\sigma_{n\mathrm{Pr}}$ = −0.144 for CH_2 at the 2-*n*-propyl group with one C_2H_5 and one H, σ_{Et} = −0.170, for CH_2 at the 2-ethyl group with one CH_3 and one H. To put it more concretely, the substituent effect, viz., abundance of electron density on the carbon (C) of the methine (CH) and methylene (CH_2) of the respective 2-alkyl groups could be expressed in the order 2-*n*-propyl < 2-ethyl ≪ 2-isopropyl, indicating that the methylene proton of the 2-*n*-

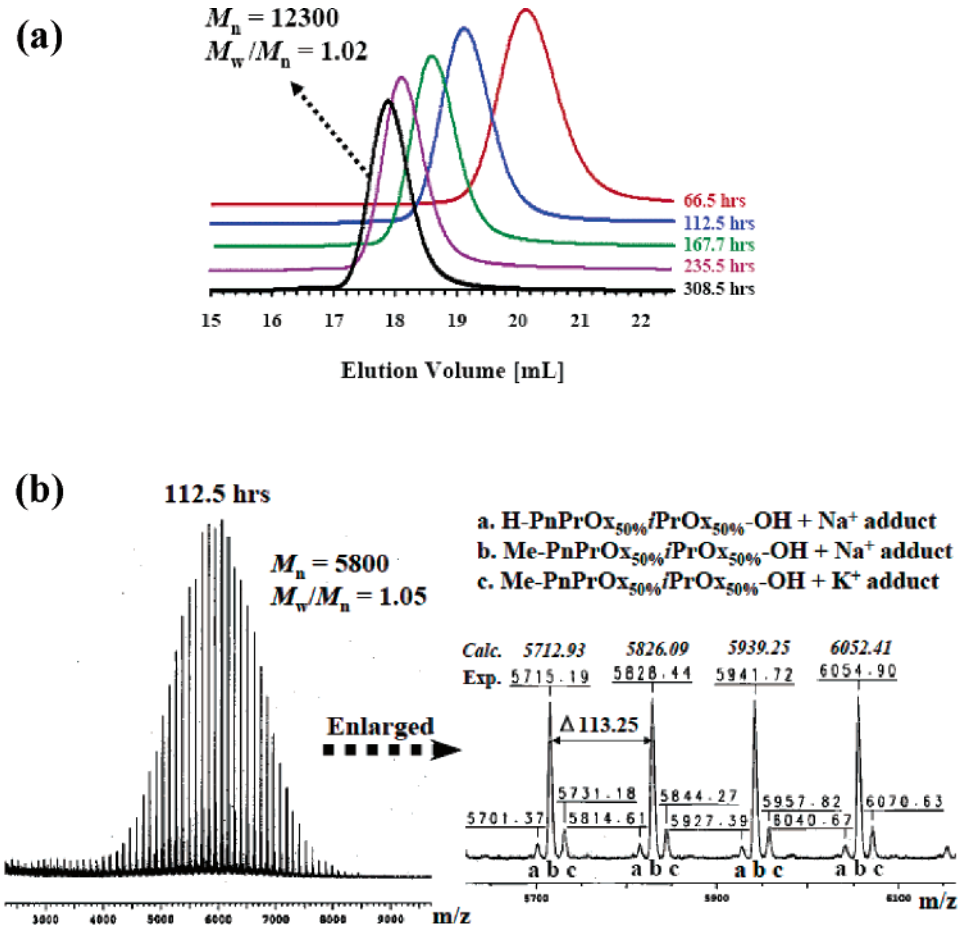

Figure 3. (a) GPC trace of P*n*PrOx$_{50\%}$*i*PrOx$_{50\%}$ copolymer samples with different molecular weights (column, G4000H$_{HR}$ and G3000H$_{HR}$; P*i*PrOx standard; eluent, DMF (containing 10 mM LiCl and 30 mM TEA); temperature, 40 °C; RI detection) and (b) MALDI−TOF mass spectrum of P*n*PrOx$_{50\%}$*i*PrOx$_{50\%}$ after 112.5 h (left) and its expanded spectrum in the mass region of 5700−6100 (right).

propyl group was most likely to be withdrawn under the same reaction conditions.

The time-dependent monomer conversion into the backbone for the respective homopolymers of *n*PrOx, *i*PrOx, and EtOx were obtained from the MALDI−TOF mass spectrometry as depicted in Figures 2 and 6, whereby the degree of polymerization (DP) was positioned on the left ordinate and the polydispersity index (PDI) (M_w/M_n) on the right ordinate. From the time-dependent DP and PDI changes of the respective homopolymers, it was obvious that the polymerization rates of both *n*PrOx and EtOx were much faster than that of *i*PrOx as well as *n*PrOx was slightly faster than EtOx. As far as the slower polymerization rate of *i*PrOx was concerned, it was reasonable to suppose that the bulky structure of the 2-isopropyl group could be sterically unfavorable for the rapid propagation.

Synthesis of Gradient Copolymers. In view of the synthetic result of the homopolymers described above, we synthesized a series of copolymers comprising *n*PrOx and *i*PrOx in order to explore the hydrophobic contribution of *n*PrOx on the LCST of the P(*n*PrOx-*grad*-*i*PrOx) copolymers (Scheme 1). The respective mixtures of 2-*n*-propyl-2-oxazoline (*n*PrOx$_{25\%}$, 5.53 mmol; *n*PrOx$_{50\%}$, 11.1 mmol; *n*PrOx$_{75\%}$, 16.6 mmol) and 2-isopropyl-2-oxazoline (*i*PrOx$_{75\%}$, 16.6 mmol; *i*PrOx$_{50\%}$, 11.1 mmol; *i*PrOx$_{25\%}$, 5.53 mmol) were added to a solution of MeOTs (0.250 mmol) in acetonitrile and polymerized at 42 °C, as in the case of the two homopolymers (P*n*PrOx and P*i*PrOx). The synthesis results of three copolymers (P*n*PrOx$_{25\%}$*i*PrOx$_{75\%}$, P*n*PrOx$_{50\%}$*i*PrOx$_{50\%}$, and P*n*PrOx$_{75\%}$*i*PrOx$_{25\%}$) with the same initial monomer/initiator ratio (DP$_{calcd}$ = 88.4) are summarized in Table 1. The polymerization behaviors of the copolymers with the initial *n*PrOx and *i*PrOx molar ratios of 25%:75%, 50%:50%, and 75%:25% were characterized by the time-dependent

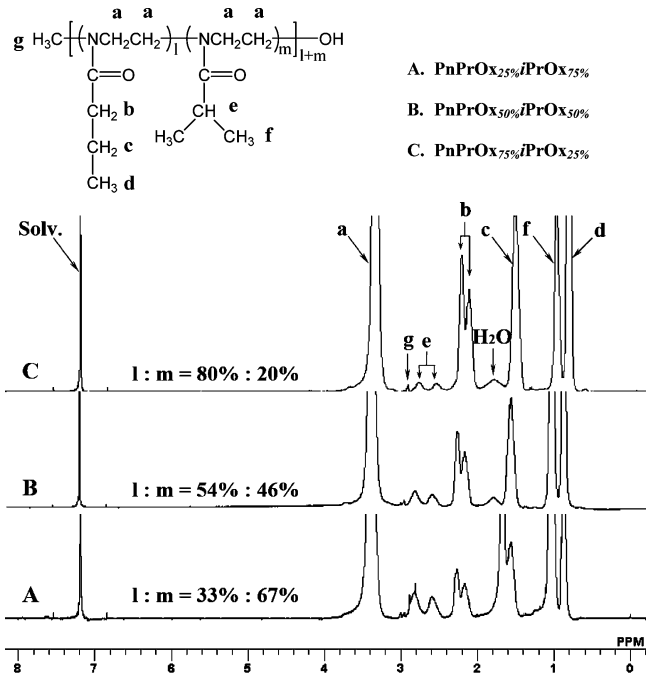

Figure 4. ^{1}H NMR spectra for the final products of three gradient copolymers (P*n*PrOx$_{25\%}$*i*PrOx$_{75\%}$, P*n*PrOx$_{50\%}$*i*PrOx$_{50\%}$, and P*n*PrOx$_{75\%}$*i*PrOx$_{25\%}$) in $CDCl_3$ at 25 °C.

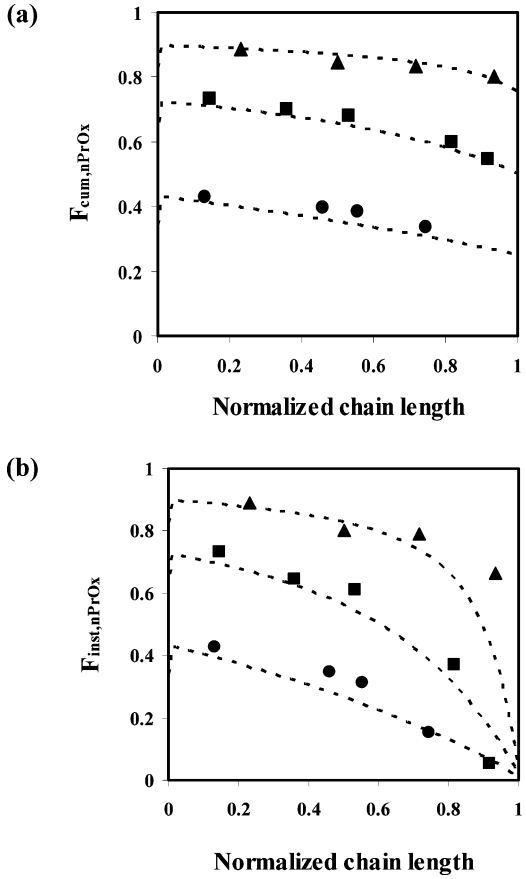

Figure 5. (a) Cumulative ($F_{cum,nPrOx}$), and (b) instantaneous ($F_{inst,nPrOx}$) composition plots for gradient copolymers. The theoretical prediction curves (dotted) were calculated using the simulation program PROCOP[17] (P*n*PrO$x_{25\%}$*i*PrO$x_{75\%}$ (●), P*n*PrO$x_{50\%}$*i*PrO$x_{50\%}$ (■), and P*n*PrO$x_{75\%}$*i*PrO$x_{25\%}$ (▲)).

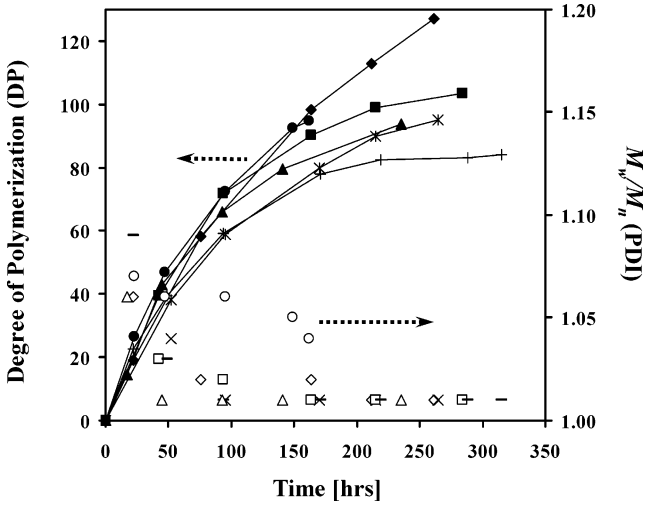

Figure 6. Degree of polymerization (DP) (left ordinate, symbols with dashed lines) and polydispersity index (PDI) (right ordinate), obtained from MALDI−TOF mass spectrometry, vs reaction time for two homopolymers (P*n*PrO*x* (●, ○), PEtO*x* (+, −)) and four random copolymers (P*n*PrO$x_{5\%}$EtO$x_{95\%}$ (∗, ×), P*n*PrO$x_{25\%}$EtO$x_{75\%}$ (♦, ◇), P*n*PrO$x_{50\%}$EtO$x_{50\%}$ (▲, △), and P*n*PrO$x_{75\%}$EtO$x_{25\%}$ (■, □)).

change in the DP and PDI via the MALDI−TOF mass and GPC traces, as seen in Figures 2 and 3. Regardless of the comonomer ratio in the feed, the experimental degree of polymerization (DP from MALDI−TOF mass spectrometry) of the respective copolymers was close to the predicted value from the initial monomer/initiator ratio (DP_{calcd} = 88.4) and their molecular weight distributions were quite narrow in all cases (Figure 2). The GPC trace of P*n*PrO$x_{50\%}$*i*PrO$x_{50\%}$, which was sampled at different polymerization times, also showed an increase in the molar mass with time and symmetrical monomodal peaks, as shown in Figure 3a. Similar results for the other two copolymers (P*n*PrO$x_{25\%}$*i*PrO$x_{75\%}$ and P*n*PrO$x_{75\%}$*i*PrO$x_{25\%}$) with different monomer ratios in the feed were also confirmed by the respective GPC traces (data not shown). Although the detailed analysis of the copolymer composition and sequence distribution for P*n*PrO$x_{50\%}$*i*PrO$x_{50\%}$ could not be done due to the same mass value between *n*PrOx and *i*PrOx ($M_{n,nPrOx} = M_{n,iPrOx}$), the end group analysis was conducted using the MALDI−TOF mass spectrum recorded after 112.5 h (Figure 3b). The most and second intense signals were assigned to the sodium and potassium adducts of Me−P*n*PrO$x_{50\%}$*i*PrO$x_{50\%}$−OH with α-methyl and *ω*-hydroxyl terminal groups, respectively, while the third intense signal was due to the sodium adduct of H−P*n*PrO$x_{50\%}$*i*PrO$x_{50\%}$−OH as a result of the undesirable proton initiation. In addition, the compositions of the final copolymer products determined by ^{1}H NMR spectrometry were almost in good agreement with the calculated values from the feed ratio of both monomers, indicating their quantitative conversion into the respective copolymers (Figure 4 and Table 1).

In this living polymerization system, copolymers were expected to have a gradient composition, providing sufficiently different reactivity ratios of the two monomers, *n*PrOx and *i*PrOx. Indeed, from the compositional analysis by ^{1}H NMR spectrometry of the respective copolymer samplings (monomer conversions: ca. 20−40%) plotted in Figure 2, the reactivity ratios of the respective monomers were calculated to be $r_{nPrOx} = 3.15$ and $r_{iPrOx} = 0.57$ using the nonlinear Tidwell−Mortimer (TM) method,[16] showing the most reasonable result for the additional composition analysis of the copolymers. Determination of the reactivity ratio at a low conversion could be affected by the different reactivity of the initiator against a specific monomer, therefore, we selected monomer conversions of ca. 20−40% as a reasonable interval in this living system of which the high polymer was not immediately formed by the reaction.[17] This difference in the reactivity ratios of the two monomers indicates that *n*PrOx should initially be consumed much faster than *i*PrOx. However, because of the decreasing concentration of the former in the residual feed, the rate of its incorporation into the polymer chain also decreased. This resulted in an increased instantaneous incorporation of *i*PrOx into the copolymer as the reaction progressed and ultimately in the formation of an *i*PrOx-rich chain end. Because of the simultaneous initiation and uniform propagation kinetics in this living system as known from the appreciably low polydispersity indices, each polymer chain should display a similar trend of a gradually decreasing *n*PrOx and an increasing *i*PrOx composition along the backbone from the α-terminal to the active *ω*-chain end. The cumulative and instantaneous composition plots ($F_{cum,nPrOx}$ and $F_{inst,nPrOx}$, respectively) vs the normalized chain length were obtained for the three copolymerizations with different initial molar ratios of *n*PrOx and *i*PrOx in the feed (Figure 5). According to the experimental plots, the shape of the obtained gradient copolymers closely followed the theoretical predictions using $r_{nPrOx} = 3.15$ and $r_{iPrOx} = 0.57$.[18] This type of methodology was useful to trace the composition drift of the gradient copolymers, as in the system of atom transfer radical copolymerization.[17]

Synthesis of Random Copolymers. On the basis of the synthetic result of two *n*PrOx and EtOx homopolymers showing similar polymerization rates, we next synthesized a series of

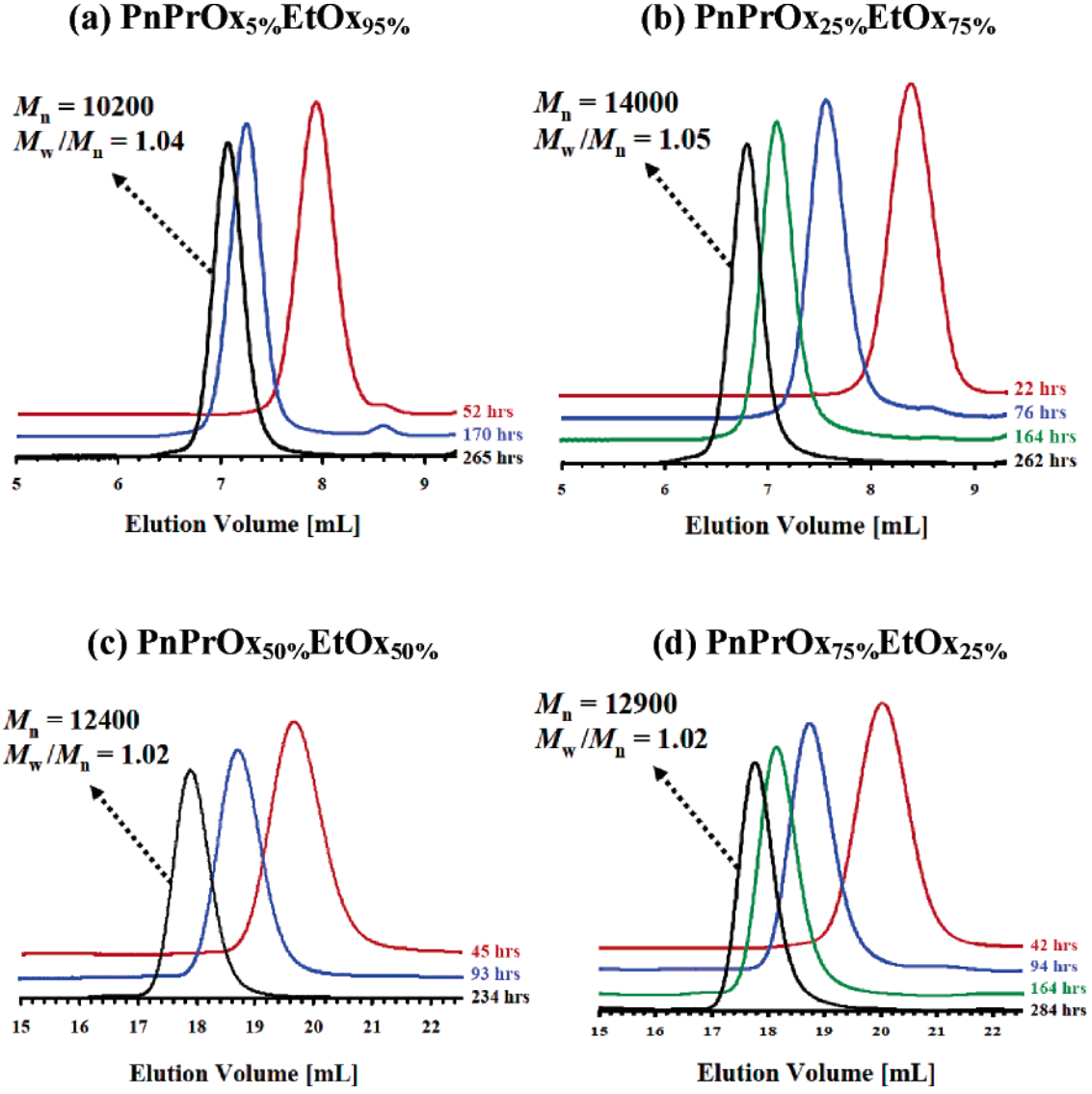

Figure 7. GPC traces of four random copolymers ((a) P*n*PrOx$_{5\%}$EtOx$_{95\%}$, (b) P*n*PrOx$_{25\%}$EtOx$_{75\%}$, (c) P*n*PrOx$_{50\%}$EtOx$_{50\%}$, and (d) P*n*PrOx$_{75\%}$-EtOx$_{25\%}$) having different molecular weights (column, SuperAW4000 and SuperAW3000 (a, b) and G4000H$_{HR}$ and G3000H$_{HR}$ (c, d); P*i*PrOx standard; eluent, DMF (containing 10 mM LiCl and 30 mM TEA); temperature, 40 °C; RI detection).

random copolymers comprising *n*PrOx and EtOx in order to explore the phase transition behavior of the P(*n*PrOx-*ran*-EtOx) copolymers without the *i*PrOx component (Scheme 1). The respective mixtures of 2-*n*-propyl-2-oxazoline (*n*PrOx$_{5\%}$, 1.11 mmol; *n*PrOx$_{25\%}$, 5.53 mmol; *n*PrOx$_{50\%}$, 11.1 mmol; *n*PrOx$_{75\%}$, 16.6 mmol) and 2-ethyl-2-oxazoline (EtOx$_{95\%}$, 21.0 mmol; EtOx$_{75\%}$, 16.6 mmol; EtOx$_{50\%}$, 11.1 mmol; EtOx$_{25\%}$, 5.53 mmol) were added to a solution of MeOTs (0.250 mmol) in acetonitrile and polymerized at 42 °C, as in the case of the two homopolymers (P*n*PrOx and PEtOx). The synthesis results of four copolymers (P*n*PrOx$_{5\%}$EtOx$_{95\%}$, P*n*PrOx$_{25\%}$EtOx$_{75\%}$, P*n*PrOx$_{50\%}$-EtOx$_{50\%}$, and P*n*PrOx$_{75\%}$EtOx$_{25\%}$) with the same initial monomer/initiator ratio (DP$_{calcd}$ = 88.4) are summarized in Table 2. The polymerization behaviors of the copolymers with the initial *n*PrOx and EtOx molar ratios of 5%:95%, 25%:75%, 50%:50%, and 75%:25% were characterized by the time-dependent change in the DP and PDI via the MALDI−TOF mass and GPC traces, as seen in Figures 6 and 7. Regardless of the comonomer ratio in the feed, the experimental degree of polymerization (DP from MALDI−TOF mass spectrometry) of the respective copolymers was close to the predicted value from the initial monomer/initiator ratio (DP$_{calcd}$ = 88.4) and their molecular weight distributions were quite narrow (Figure 6). The GPC traces of the four copolymers with different monomer ratios in the feed (P*n*PrOx$_{5\%}$EtOx$_{95\%}$, P*n*PrOx$_{25\%}$EtOx$_{75\%}$, P*n*PrOx$_{50\%}$EtOx$_{50\%}$, and P*n*PrOx$_{75\%}$EtOx$_{25\%}$), which were sampled at different polymerization times, also showed an increase in the molar mass with time and symmetrical monomodal peaks, as shown in Figure 7a−d. In addition, the compositions of the final copolymer products determined by ^{1}H NMR spectrometry were almost in good agreement with the calculated values from the feed ratio of both monomers, indicating their quantitative conversion into the respective copolymers (Figure 8 and Table 2).

In this living polymerization system, the copolymers were expected to form a random composition, providing similar reactivity ratios of the two monomers, *n*PrOx and EtOx. Indeed, from the composition analysis by ^{1}H NMR spectrometry of the respective copolymer samplings (monomer conversions: ca. 20−40%) plotted in Figure 6, the reactivity ratios of the respective monomers were calculated to be $r_{n\mathrm{PrOx}}$ = 1.28 and r_{EtOx} = 1.04 using the nonlinear Tidwell−Mortimer (TM) method.[16] This similarity in the reactivity ratios of two monomers indicates that both *n*PrOx and EtOx should be introduced into the copolymer backbone at almost an equal rate. Because of the simultaneous initiation and uniform propagation

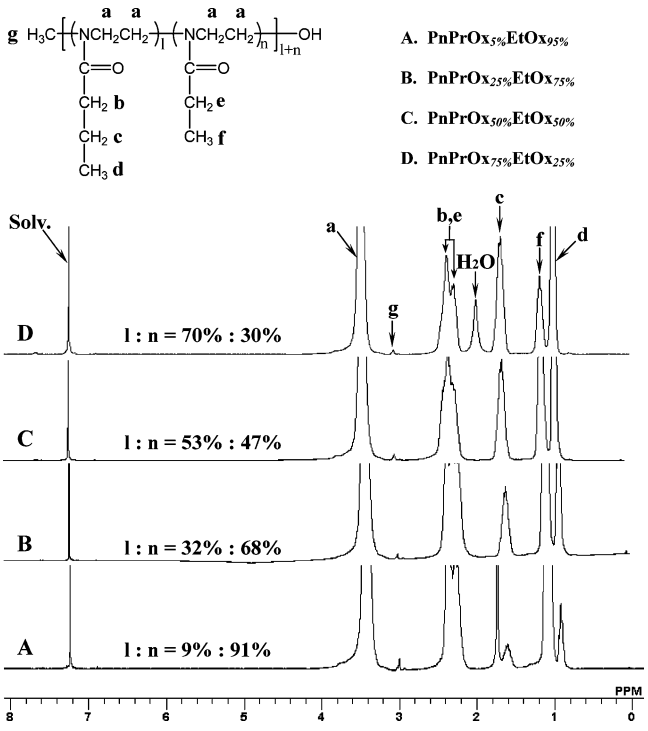

Figure 8. ^{1}H NMR spectra for the final products of the four random copolymers (P*n*PrOx$_{5\%}$EtOx$_{95\%}$, P*n*PrOx$_{25\%}$EtOx$_{75\%}$, P*n*PrOx$_{50\%}$EtOx$_{50\%}$, and P*n*PrOx$_{75\%}$EtOx$_{25\%}$) in $CDCl_3$ at 25 °C.

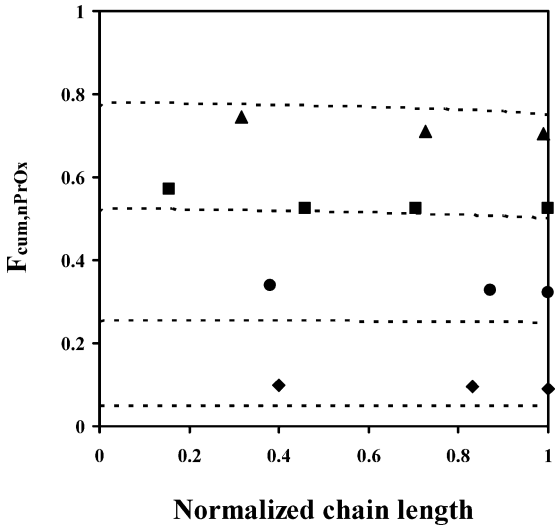

Figure 9. Cumulative ($F_{cum,nPrOx}$) composition plots for random copolymers. The theoretical prediction curves (dotted) were calculated using the simulation program PROCOP[17] (P*n*PrOx$_{5\%}$EtOx$_{95\%}$ (◆), P*n*PrOx$_{25\%}$EtOx$_{75\%}$ (●), P*n*PrOx$_{50\%}$EtOx$_{50\%}$ (■), and P*n*PrOx$_{75\%}$EtOx$_{25\%}$ (▲)).

kinetics in this living system as known from the extremely low polydispersity indices, each polymer chain should exhibit a similar composition ratio of *n*PrOx and EtOx along the backbone from the α-terminal to active ω-chain end. The cumulative composition plots ($F_{cum,nPrOx}$) vs the normalized chain length were obtained for the four copolymerizations with different initial molar ratios of *n*PrOx and EtOx in the feed (Figure 9). According to the experimental plots, the shape of the obtained random copolymers almost followed the theoretical curves using $r_{nPrOx} = 1.28$ and $r_{iPrOx} = 1.04$.[18]

In addition, a series of MALDI−TOF mass spectra for P*n*PrOx$_{50\%}$EtOx$_{50\%}$, which were sampled at different polymerization times, were obtained as shown in Figure 10, showing a good coincidence with the result of the GPC trace. The MALDI−TOF mass spectrometry thus provided quantitative information about the sequence and composition present in the copolymer when compared to the theoretical mass values and relative intensities for a specific copolymer with the experimental mass spectrum.[19] The series of all the copolymer samplings with the chain lengths below ca. $M_n = 10\,000$ could provide comparatively clearer mass spectra, and the enlarged mass spectrum of P*n*PrOx$_{50\%}$EtOx$_{50\%}$ sampled after 17 h was selected for a detailed analysis of copolymer composition and sequence distribution (Figure 10). All the peaks shown in the mass spectrum of Figure 10 were assigned to copolymers comprised of the *n*PrOx and EtOx monomer units with both methyl groups at the α-terminals and hydroxyl groups at the ω-terminals. The calculated mass of each copolymer was expressed by the following equation:

$$\begin{aligned}\text{Mass}_{\text{calcd}} &= [n\text{PrOx}]_{l-\text{mers}} + [\text{EtOx}]_{n-\text{mers}} \\ &= \Delta[n\text{PrOx}]l + \Delta[\text{EtOx}]n + [\alpha\text{-methyl and} \\ &\quad \omega\text{-hydroxyl groups}] + [\text{Na}^+]\end{aligned}$$

($\text{Mass}_{\text{calcd}}(m/z)$; the calculated mass of a copolymer with the degree of polymerization nearest to the measured value, Δ[*n*PrOx] (or Δ[EtOx]); the mass of the monomer unit, [Na^+]; the mass of sodium ion.) The detailed peak assignments are summarized in Table 3 in which $\text{Mass}_{\text{expt}}$ is the experimental mass value of the most and second intense signals among the respective homologue series in the mass region of 1200−1900. For instance, the strongest signal ($\text{Mass}_{\text{expt}} = 1554.36$) and second most intense signal ($\text{Mass}_{\text{expt}} = 1540.12$) in the mass region of 1500−1600 almost agreed with the calculated mass values of the two corresponding copolymers as shown below.

$$[n\text{PrOx}]_{8-\text{mers}} + [\text{EtOx}]_{6-\text{mers}} = 113.158 \times 8 + 99.13 \times 6 + 32.042 + 22.99 = 1555.08$$

$$[n\text{PrOx}]_{7-\text{mers}} + [\text{EtOx}]_{7-\text{mers}} = 113.158 \times 7 + 99.13 \times 7 + 32.042 + 22.99 = 1541.05$$

Similar results for the other three random copolymers (P*n*PrOx$_{5\%}$EtOx$_{95\%}$, P*n*PrOx$_{25\%}$EtOx$_{75\%}$, and P*n*PrOx$_{75\%}$EtOx$_{25\%}$) with different monomer ratios in the feed were also confirmed by MALDI−TOF mass spectrometry (data not shown).

Determination of the Cloud Points (T_{cp}). The measurement of a 10% decrease point in optical transmittance, defined here as the cloud points (T_{cp}), was adapted to determine the lower critical solution temperature (LCST) of a polymer solution.

Figure 11a showed the dependence of the turbidity on the increasing temperature for the (co)polymer solutions with the different compositions between *n*PrOx and *i*PrOx. The transmittance sharply decreased at a specific temperature in phosphate-buffered solution (10 mM PBS (pH = 7.4)), indicating a sharp LCST-type phase transition. The LCST values of P(*n*PrOx-*grad*-*i*PrOx) were found to linearly decrease with the increasing mole% of *n*PrOx (l), from 38.7 °C at $l = 0\%$ to 23.8 °C at $l = 100\%$ for a 1.0 wt % polymer solution (Figure 11b). Regardless of the *n*PrOx to *i*PrOx ratio, an exceedingly clear sensitivity of the phase separation was observed in all cases (Table 1). Although P(*n*PrOx-*grad*-*i*PrOx) has a compositional gradient along the copolymer strand, a notable point to emphasize about this turbidimetric result is that the observed transition behavior was appreciably sharp and simply connected to the composition ratio of both monomers in the copolymers. Of special interest was the P*n*PrOx homopolymer independently exhibiting a sharp

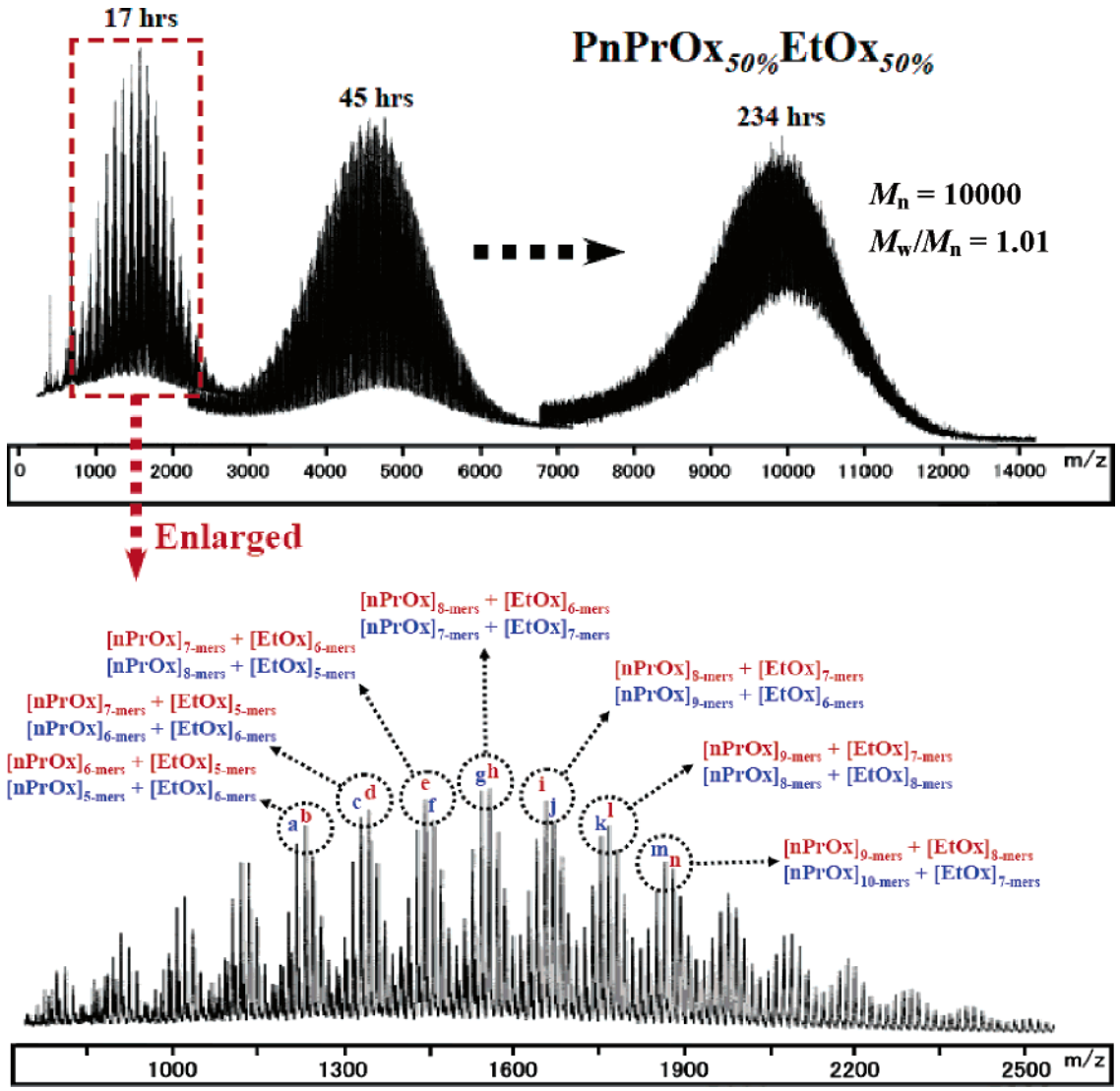

Figure 10. MALDI−TOF mass spectra of random copolymer samples comprising *n*PrOx$_{50\%}$ and EtOx$_{50\%}$ after 17, 45, and 234 h (upper), and enlarged detail in the mass region of 700−2500 for the first sampling P*n*PrOx$_{50\%}$EtOx$_{50\%}$ after 17 h (lower).

Table 3. Assignment of MALDI-TOF Mass Spectral Peaks Shown in Figure 10

$mass_{exp}$	$mass_{calc}$	assignment	$mass_{exp}$	$mass_{calc}$	assignment
1213.92	1215.60	a. $[nPrOx]_{5\text{-mers}} + [EtOx]_{6\text{-mers}}$	1227.96	1229.63	b. $[nPrOx]_{6\text{-mers}} + [EtOx]_{5\text{-mers}}$
1327.49	1328.76	c. $[nPrOx]_{6\text{-mers}} + [EtOx]_{6\text{-mers}}$	1341.52	1342.79	d. $[nPrOx]_{7\text{-mers}} + [EtOx]_{5\text{-mers}}$
1455.19	1455.95	f. $[nPrOx]_{8\text{-mers}} + [EtOx]_{5\text{-mers}}$	1440.96	1441.92	e. $[nPrOx]_{7\text{-mers}} + [EtOx]_{6\text{-mers}}$
1540.12	1541.05	g. $[nPrOx]_{7\text{-mers}} + [EtOx]_{7\text{-mers}}$	1554.36	1555.08	h. $[nPrOx]_{8\text{-mers}} + [EtOx]_{6\text{-mers}}$
1667.71	1668.23	j. $[nPrOx]_{9\text{-mers}} + [EtOx]_{6\text{-mers}}$	1653.53	1654.21	i. $[nPrOx]_{8\text{-mers}} + [EtOx]_{7\text{-mers}}$
1752.64	1753.34	k. $[nPrOx]_{8\text{-mers}} + [EtOx]_{8\text{-mers}}$	1766.76	1767.36	l. $[nPrOx]_{9\text{-mers}} + [EtOx]_{7\text{-mers}}$
1880.17	1880.522	m. $[nPrOx]_{10\text{-mers}} + [EtOx]_{7\text{-mers}}$	1865.95	1866.49	n. $[nPrOx]_{9\text{-mers}} + [EtOx]_{8\text{-mers}}$

LCST behavior near room temperature. The LCST (23.8 °C) of P*n*PrOx with a more hydrophobic 2-*n*-propyl side group was lower by a large margin compared to that (62−65 °C) of the PEtOx high polymers, but almost constant regardless of the increasing molecular weight and concentration (data not shown). In addition, the LCST of P*n*PrOx was also lower than that (38.7 °C) of P*i*PrOx, a chemical isomer of P*n*PrOx. This difference in LCST (Δ = 14.9 °C) between P*n*PrOx and P*i*PrOx could be explained by the similar trend between PNiPAAm and poly(*N*-*n*-propylacrylamide) (PNnPAAm), viz., the lower LCST of PNnPAAm than PNiPAAm is ascribed to a reduced solvent accessible area of the linear *n*-propyl group against the branched isopropyl group.[20]

Similarly, Figure 12a shows the dependence of the turbidity on the increasing temperature for the (co)polymer solutions with the different compositions between *n*PrOx and EtOx. The transmittance sharply decreased at a specific temperature in phosphate-buffered solution (10 mM PBS (pH = 7.4)). The LCST values of P(*n*PrOx-*ran*-EtOx) increased linearly with decreasing the content of *n*PrOx to 32 mol % from 23.8 °C at

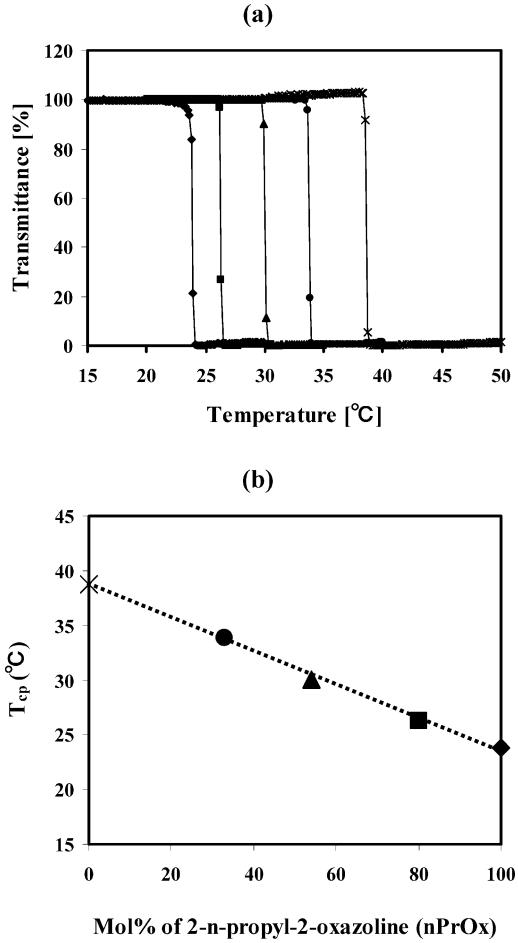

Figure 11. (a) Transmittance changes at 500 nm of 1.0 wt % gradient (co)polymer solutions (P*n*PrOx (◆), P*n*PrOx$_{25\%}$*i*PrOx$_{75\%}$ (●), P*n*PrOx$_{50\%}$*i*-PrOx$_{50\%}$ (▲), P*n*PrOx$_{75\%}$*i*PrOx$_{25\%}$ (■), and P*i*PrOx (×)) as a function of temperature (10 mM PBS (pH = 7.4); rate, 0.5 °C/min). (b) Relationship between cloud point (T_{cp}) and composition in the P(*n*PrOx-*grad*-*i*PrOx) (co)polymers.

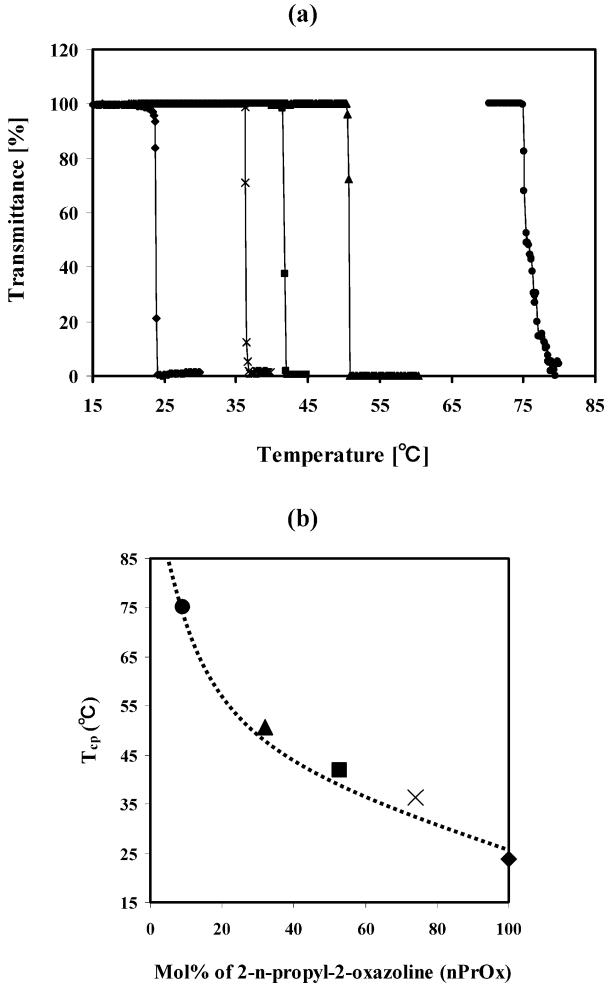

Figure 12. (a) Transmittance changes at 500 nm of 1.0 wt % random (co)polymer solutions (P*n*PrOx (◆), P*n*PrOx$_{5\%}$EtOx$_{95\%}$ (●), P*n*PrOx$_{25\%}$-EtOx$_{75\%}$ (▲), P*n*PrOx$_{50\%}$EtOx$_{50\%}$ (■), P*n*PrOx$_{75\%}$EtOx$_{25\%}$ (×)) as a function of temperature (10 mM PBS (pH = 7.4); rate, 0.5 °C/min). (b) Relationship between cloud point (T_{cp}) and composition in the P(*n*PrOx-*ran*-EtOx) (co)polymers.

l = 100% to 50.6 °C at l = 32% for a 1.0 wt % polymer solution, but progressively increased in the region below l = 32% approaching to 75.1 °C at l = 9% (Figure 12b). No observable change in the transmittance appeared in the case of a 100% PEtOx homopolymer ($M_{n,GPC}$ = 8000, $M_{n,TOF-MS}$ = 8300) as previously described.[9] Regardless of the *n*PrOx to EtOx ratio, an exceedingly clear sensitivity of the phase separation was observed with the increasing temperature in all cases (Table 2).

It may be reasonable to assume that the LCST property of such a gradient copolymer as P(*n*PrOx-*grad*-*i*PrOx) may become more complicated than P(*n*PrOx-*ran*-EtOx) with a simple random composition, due to the possible formation of a micelle-like molecular association derived from a deviating amphiphilicity along the polymer strand. Thus, P(*n*PrOx-*ran*-EtOx) could be ideal for a wide range of LCST tunings rather than P(*n*PrOx-*grad*-*i*PrOx), unless there is a specific application to target the gradient copolymer. Nevertheless, the static light scattering (SLS) measurements of P(*n*PrOx-*grad*-*i*PrOx) with varying temperatures provided no obvious evidence of the multimolecular association such as micelle structures, as in the P(*i*PrOx-*grad*-EtOx) system (data not shown). Although we may not exclude the possibility of different hydration states between the gradient and random copolymers below the LCST due to the distinct structure and composition of the two monomers incorporated in the respective copolymer strand, the turbidimetric behaviors of both copolymers followed a simple and practical rule correlated to the molar ratio of both monomers. Detailed solution behaviors of these gradient and random copolymers including the P*n*PrOx homopolymer should be an important topic for further study to understand their fundamental molecular dynamics related to temperature changes, but we recall that the present study focused on the well-defined Ox polymerization as a convenient synthetic route to selectively obtain the gradient or random copolymers with finely tuned LCSTs.

Conclusions

This study established the facile and selective synthetic route of thermosensitive POx gradient or random copolymers via the living cationic process between *n*PrOx and *i*PrOx (or EtOx). The respective monomer reactivity ratios were found to be 3.15 and 0.57 for *n*PrOx and *i*PrOx, respectively, sufficiently different to form the gradient copolymers P(*n*PrOx-*grad*-*i*PrOx), and 1.28 and 1.04 for *n*PrOx and EtOx, respectively, appropriate to obtain the random copolymers P(*n*PrOx-*ran*-EtOx). Turbidity measurements revealed that the LCST of both the gradient and random copolymers could be precisely tuned over a broad range of temperatures by varying the molar ratio of the two Ox monomers. This methodology of copolymerizing a variety of Ox monomers with different hydrophobic and hydrophilic balances, apparently lead to the systematic preparation of a series

of well-defined gradient and random POx copolymers with finely tuned LCSTs. Most of all, P(*n*PrOx-*ran*-EtOx) with a simple random sequence in the backbone showed a rapid and modulated response to the temperature change from 23.8 to 75.1 °C, considered the most ideal system for tuning the LCST around the physiological condition. These POx (co)polymers also have a promising use in biomedical applications, such as the preparation of thermosensitive bioconjugates and drug delivery systems via the synthesis of biofunctional block or graft copolymers.

Acknowledgment. This work was financially supported by the Special Coordination Funds for Science and Technology from the Ministry of Education, Culture, Sports, Science, and Technology of Japan (MEXT) as well as by the Core Research for Evolutional Science and Technology (CREST) from the Japan Science and Technology Agency (JST). The authors are also grateful to Prof. T. Tsuruta, Professor Emeritus, The University of Tokyo, for his valuable discussions and critical comments on this research.

References and Notes

(1) (a) Bergbreiter, D. E.; Osburn, P. L.; Wilson, A.; Sink, E. M. *J. Am. Chem. Soc.* **2000**, *122*, 9058. (b) Hamamoto, H.; Suzuki, Y.; Yamada, Y.; Tabata, H.; Takahashi, H.; Ikegami, S. *Angew. Chem., Int. Ed.* **2005**, *44*, 4536.

(2) (a) Uchiyama, S.; Kawai, N.; de Silva, A. P.; Iwai, K. *J. Am. Chem. Soc.* **2004**, *126*, 3032. (b) Hu, Z. B.; Chen, Y. Y.; Wang, C. J.; Zheng, Y. D.; Li, Y. *Nature*, **1998**, *393*, 149.

(3) (a) Kanazawa, H.; Yamamoto, K.; Matsushima, Y.; Takai, N.; Kikuchi, A.; Sakurai, Y.; Okano, T. *Anal. Chem.* **1996**, *68*, 100. (b) Kikuchi, A.; Okano, T. *Prog. Polym. Sci.* **2002**, *27*, 1165.

(4) (a) Stayton, P. S.; Shimoboji, T.; Long, C.; Chilkoti, A.; Chen, G.; Harris, J. M.; Hoffman, A. S. *Nature (London)* **1995**, *378*, 472. (b) Matsukata, M.; Aoki, T.; Sanui, K.; Ogata, N.; Kikuchi, A.; Sakurai, Y.; Okano, T. *Bioconjugate Chem.* **1996**, *7*, 96. (c) Ding, Z.; Chen, G.; Hoffman, A. S. *J. Biomed. Mater. Res.* **1998**, *39*, 498.

(5) (a) Yoshida, R.; Sakai, T.; Okano, T.; Sakurai, Y.; Bae, Y. H.; Kim, S. W. *J. Biomater. Sci. Polym. Ed.* **1991**, *3*, 155. (b) Cammas, S.; Suzuki, K.; Sone, Y.; Kakurai, Y.; Kataoka, K.; Okano, T. *J. Controlled Release.* **1997**, *48*, 157. (c) Kono, K. *Adv. Drug. Deliv. Rev.* **2001**, *53*, 307.

(6) (a) Park, J. S.; Akiyama, Y.; Winnik, F. M.; Kataoka, K. *Macromolecules* **2004**, *37*, 6786. (b) Diab, C.; Akiyama, Y.; Kataoka, K.; Winnik, F. M. *Macromolecules* **2004**, *37*, 2556.

(7) (a) Heskins, M.; Guillet, J. E. *J. Macromol. Sci. Chem.* **1968**, *A2*, 1441. (b) Schild, H. G. *Prog. Polym. Sci.* **1992**, *17*, 163.

(8) Park, J. S.; Akiyama, Y.; Yamasaki, Y;, Kataoka, K. *Langmuir* **2007**, *23*, 138.

(9) Park, J. S.; Kataoka, K. *Macromolecules* **2006**, *39*, 6622.

(10) (a) Kobayashi, S. *Prog. Polym. Sci.* **1990**, *15*, 751. (b) Aoi, K.; Okada, M. *Prog. Polym. Sci.* **1996**, *21*, 151. (c) Kobayashi, S.; Uyama, H. *J. Polym. Sci., Part A: Polym. Chem.* **2002**, *40*, 192.

(11) (a) Chiu, T. T.; Thill, B. P.; Fairchok, W. J. In *Water-Soluble Polymers*; Advances in Chemistry Series 213; Glass, J. E., Ed.; American Chemical Society: Washington, DC, 1986; pp 425−433. (b) Lin, P.; Pearce, E. M.; Kwei, T. K. *J. Polym. Sci., Part B: Polym. Phys.* **1988**, *26*, 603.

(12) Chujo, Y.; Sada, K.; Matsumoto, K.; Saegusa, T. *Macromolecules* **1990**, *23*, 1234.

(13) Perrin, D. D.; Armarego, W. L. F.; Perrin, D. R. *Purification of Laboratory Chemicals*; Pergamon: Oxford, U.K., 1980.

(14) (a) Levy, A.; Litt, M. *J. Polym. Sci., Part A-1* **1968**, *6*, 1883. (b) Litt, M.; Levy, A.; Herz, J. *J. Macromol. Sci., Chem.* **1975**, *A9*, *703*. (c) Warakomski, J. M.; Thill, B. P. *J. Polym. Sci., Part, A.* **1990**, *28*, 3551.

(15) Hammett, L. P. *J. Am. Chem. Soc.* **1937**, *59*, 96.

(16) Tidwell, P. W.; Mortimer, G. A. *J. Macromol. Sci. Rev. Macromol. Chem.* **1970**, *C4*, 281.

(17) (a) Pakula, T.; Matyjaszewski, K. *Macromol. Theory Simul.* **1996**, *5*, 987. (b) Matyjaszewski, K.; Ziegler, M. J.; Arehart, S. V.; Greszta, D.; Pakula, T. *J. Phys. Org. Chem.* **2000**, *13*, 775. (c) Madruga, E. L. *Prog. Polym. Sci.* **2002**, *27*, 1879.

(18) Hagipol, C. *Copolymerization-Toward a Systematic Approach*; Kluwer Academic: New York, 1999.

(19) (a) Montaudo, M. S. *Rapid Commun. Mass Spectrom.* **1999**, *13*, 639. (b) Montaudo, M. S. *Mass Spectrom. Rev.* **2002**, *21*, 108.

(20) Mao, H.; Li, C.; Zhang, Y.; Furyk, S.; Cremer, P. S.; Bergbreiter, D. E. *Macromolecules* **2004**, *37*, 1031.

MA0701181